

Fundamental approaches for the application of pineapple leaf fiber in high performance reinforced composites

M. Siti Alwani¹⁾, Abdul Khalil^{1), 2), *)}, Md Nazrul Islam^{1), 3)}, W.O. Wan Nadirah¹⁾, Rudi Dungani^{1), 4)}

DOI: dx.doi.org/10.14314/polimery.2014.798

Abstract: The fundamental understanding of fibers, because of their polymeric nature, helps to improve the properties of the final product. This study presents an approach to examine the morphology, anatomy, cell wall architecture and distribution of lignin from pineapple leaf fiber by light microscopy, scanning electron microscopy with energy dispersive X-ray, transmission electron microscopy and Raman spectroscopy. Light microscopy and scanning electron microscopy revealed that the vascular bundle was randomly distributed across the transverse section of the pineapple leaf consisting of sclerenchyma, vessel, phloem and parenchyma cells. The fiber surface was covered with a rough hydrophobic layer composed of cutin, lignin, silica, waxes and a mixture of other cell wall materials. TEM investigations revealed the nanocomposite structure of the cell wall that were composed of typical primary and secondary cell wall layers. The topochemical distribution of lignin confirmed that the concentration of lignin at the cell corners was higher compared to compound middle lamella and secondary walls. This study helps to understand the fundamentals of the pineapple leaf fiber and can also help in the design of improved bio-based materials.

Keywords: pineapple leaf fiber, surface morphology, anatomy, cell wall, biocomposites.

Podstawowa ocena włókien liści ananasa jako wzmocnienia w biokompozytach

Streszczenie: Omówiono podstawowe badania włókien liści ananasa przeprowadzone metodami: mikroskopii świetlnej, skaningowej mikroskopii elektronowej z rozpraszaniem energii promieniowania rentgenowskiego, transmisyjnej mikroskopii elektronowej oraz spektroskopii Ramana. Badania obejmowały morfologię, architekturę komórki, oraz zawartość i rozkład ligniny w liściu. Mikroskopia świetlna i skaningowa mikroskopia elektronowa wykazały, że wiązki naczyniowe są losowo rozłożone w przekroju poprzecznym liścia ananasa i składają się z komórek sklerenchymii, naczyń łyka i komórek miąższu. Powierzchnię włókien pokrywa rogowa warstwa hydrofobowa, złożona z ligniny, krzemionki, wosków i mieszaniny innych materiałów ścianek komórkowych. Badania potwierdziły nanokompozytową strukturę ściany komórkowej, którą stanowią typowe warstwy ścian komórkowych pierwotnych i wtórnych. Stężenie ligniny w narożach komórek było większe niż w środku lameli i ścianie wtórnej. Przeprowadzone badania umożliwiają zrozumienie budowy i wynikających z niej właściwości włókien liści ananasa i ułatwiają projektowanie polimerowych biokompozytów z udziałem takich włókien.

Słowa kluczowe: włókna liści ananasa, morfologia powierzchni liścia, budowa anatomiczna, ściana komórkowa, biokompozyty.

The growing concern over increasing fossil fuel prices, global warming issues and greenhouse effects have

stimulated a tremendous interest in the use of renewable materials that are compatible with the environment. Biomass is a readily available and low-cost feedstock that effectively stores energy, carbon, oxygen, and hydrogen from the environment *via* photosynthesis. Biomass feedstocks are one of the few resources that can facilitate the large-scale, sustainable production of the substantial volumes of energy and materials needed to support the world's population and supplement non-renewable raw materials [1]. Recent advances in plant fiber development, genetic engineering and composite science offer significant opportunities for an exploration and development of improved materials from renewable resources for applications in biocomposites, pulp and paper, auto-

¹⁾ Universiti Sains Malaysia, School of Industrial Technology, 11800, Penang, Malaysia.

²⁾ Universiti Putra Malaysia, Institute of Tropical Forestry and Forest Products (INTROP), Department of Biocomposite Technology, 43400 UPM Serdang, Selangor, Malaysia.

³⁾ Khulna University, School of Life Science, Khulna — 9208, Bangladesh.

⁴⁾ Institut Teknologi Bandung, School of Life Sciences and Technology, Gedung Labtex XI, Jalan Ganesha 10, Bandung 40132, West Java-Indonesia.

^{*)} Author for correspondence; e-mail: akhalilhps@gmail.com

motive, medical, packaging, construction, aerospace, marine, electronics, pharmaceutical and biomass energy production [2]. However, biodegradation is a major challenge for these fibers along with the isolation, yield, forage digestibility or polysaccharide saccharifiability. The reduction of lignin content in plant feed stocks, or facilitation of its removal, is also a major interest in the field of lignocellulosic biofuels and pulping [3].

In response to meeting the global demand to produce an adequate volume of materials at sufficiently low cost, research must first address several issues including, but not limited to, understanding plant cell wall biosynthesis and its structure in the context of biomass recalcitrance; development time, energy, and material-efficient conversion technologies. Various methods and techniques have been developed over the past few years to analyze the cell wall characteristics and lignin distribution for different plants including light microscopy [4, 5], scanning electron microscopy in conjunction with energy dispersive X-ray analysis and transmission electron microscopy [6–8]. Recently, Raman spectroscopy applications have improved dramatically as a sensitive and non-destructive tool for chemical profiling of plants, including quantification of lignin distribution in plant cell wall [9–11]. Agarwal *et al.* [12] reported that this method was capable of providing a rapid, direct and accurate measure of chemical substances present in plants.

Among many agricultural residues, pineapple (*Ananas comosus* Merr.) leaves are common in tropical and sub-tropical regions, which need global attention for its commercial exploration. Pineapple plants are widely cultivated and focused only for its delicious and fragrant fruits leaving the leaves, a major part of the plant, mainly for compost or fuel. Fibers can be extracted from the leaves that have high cellulose contents and are mechanically sound as a reinforcement for polymer composites [13]. It has also suitable textile properties and is capable of blending with jute, cotton, ramie and some other synthetic fibers [14]. Despite being mechanically excellent and environmentally sound, pineapple leaf fibers (PALF) are the least-studied of the above-mentioned natural fibers, especially for reinforcing composites [15, 16]. Moreover, most of the works are concentrated mainly on the utilization without thoroughly knowing the properties. Thus, a systematic investigation on the cell wall structure and lignin distribution of PALF is a pressing demand for its' efficient exploration. Considering these facts, this study was undertaken to understand the plant cell wall structure and lignin distribution in cell walls, which would lead to diversified uses of this abundantly available renewable resource for different applications. Light microscopy (LM), scanning electron microscopy (SEM) and transmission electron microscopy (TEM) were used to study the anatomical and ultrastructural characteristics of the fiber cell wall. Raman spectroscopy was employed to acquire spectra maps and chemical images of the cell wall cross-sections. Scanning electron microscopy with ener-

gy dispersive X-ray (SEM-EDX) was used to reveal the variation in lignin content in the cell walls.

EXPERIMENTAL

Material

Pineapple leaves at the age of 6 months were obtained from a commercial farm in Penang, Malaysia. Specimens were taken from the leaf and dissected into small blocks. These blocks were preserved in ethanol and glycerin (1:1 v/v) until used.

Methods of testing

Light microscopy (LM)

Small, fresh samples were dehydrated in an ethanol series and embedded in Spur's resin. The samples were polymerized for 24 h at 60 °C. The transverse sections (TS) (1 µm) were cut from the embedded material using a Sorvall ultra microtome (MT 500, Japan) and stained with 0.05 % toluidine blue. The stained sections were viewed under a polarized light microscope (Olympus BX50, Japan).

Scanning electron microscopy (SEM)

Blocks of 1–2 mm³ were prepared from pineapple leaf tissue with razor blades. The sample was air dried and gold coated by a sputter coater. The resulting blocks were then examined by a SEM (Hitachi S-3000N, Japan) under high vacuum.

Scanning electron microscopy with energy dispersive X-ray (SEM-EDX)

Free-hand, transversely cut sections of 3 mm thickness were extracted with a mixture of acetone-ethanol (2:1 v/v) for 24 h and then dehydrated with graded ethanol. Subsequently, they were reacted with 1 % potassium permanganate (KMnO₄) for 10 min at room temperature and air-dried. The lignin distribution was measured by a Hitachi S-3400N SEM-EDXA after being coated with a 10-nm thick gold film. The accelerating voltage and probe current were 20 kV and 80 µA, respectively. Point scans were used to examine the lignin distribution in different morphological regions of the plant fibers. The point analysis of Mn-K X-rays was performed with a Horiba Si (Li) energy-dispersive spectrometer.

Raman spectroscopy

PALF cross sections (5 µm) were put on a glass slide with a drop of water covered by a cover slip (0.17 mm thickness) and sealed with nail-polish to avoid evaporation. Raman spectra were acquired with Raman and Photo-

luminescence Spectroscopy (Horiba Jobin Yvon) equipped with a confocal microscope (Olympus BX51, Japan). A linear-polarized 514-nm laser excitation was focused with a diffraction-limited spot size ($1.22 \lambda/\text{NA}$). LabSpec software was used for the data processing where the baseline of the spectra was corrected and smoothed using the Savitsky–Golay algorithm. Average spectra were calculated for different cell wall layers (CC, CML and SW) by marking a distinct area under the microscope image.

Transmission electron microscopy (TEM)

Samples were dehydrated in an ethanol series followed by acetone and embedded in Spur's resin. Ultrathin sections (0.1 mm) were cut with a diamond knife and placed on copper grids. Samples were stained with uranyl acetate and Reynolds's lead citrate. The grids were observed on a Hitachi H-600 transmission electron microscope (TEM) at 75 kV.

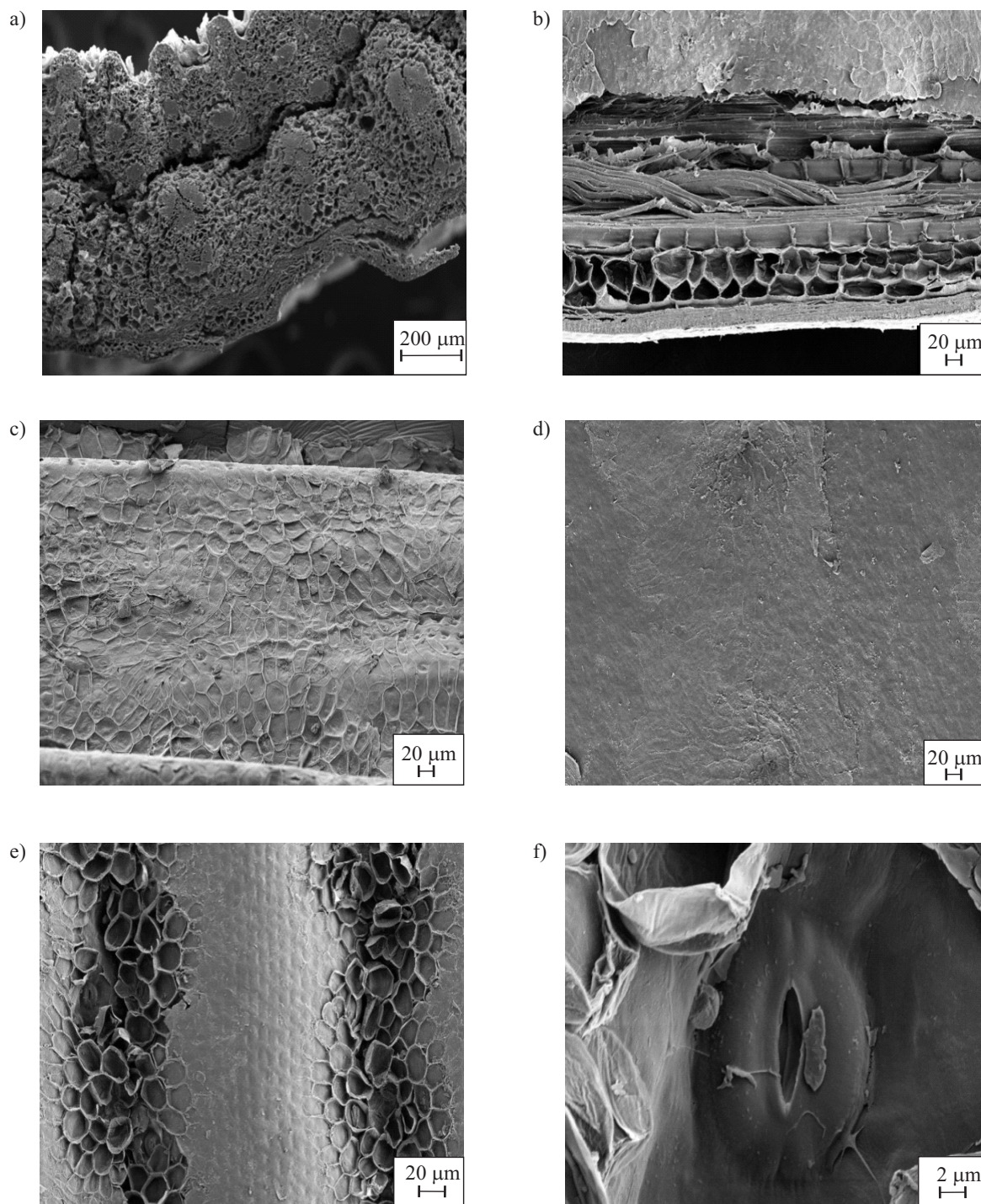


Fig. 1. SEM micrographs of PALF through different sections: a) transverse section (73 \times), b) longitudinal section (200 \times), c) abaxial surface (225 \times), d) adaxial surface (650 \times), e) stomata on abaxial surface (200 \times), f) stoma in face view (2000 \times)

RESULTS AND DISCUSSION

Morphological characteristics

Figure 1 shows the SEM micrograph of transverse, longitudinal and surface views of pineapple leaf. A thick epidermis layer that acts as a protective cover is seen on the periphery of the leaf at cross section (Fig. 1a). Beneath the epidermis, there is a loose layer containing parenchyma and vascular bundles that are randomly scattered across the leaf. The longitudinal surface shows a multicellular nature with an overlap of cells like in other natural fibers (Fig. 1b). The nodes are at irregular distances, which divide the fiber into individual cells. Figure 1c and

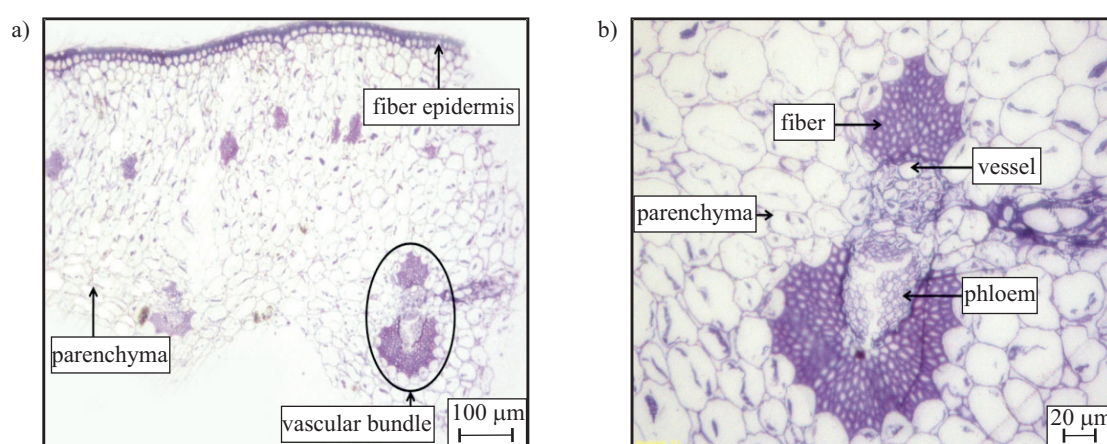


Fig. 2. Transverse section of pineapple leaf: a) 10 \times , b) 40 \times

1d shows the abaxial (lower) and adaxial (upper) view of the leaf, respectively. Figure 1d demonstrates that the leaf has a very thin and flat structure that allows an efficient penetration of light for the photosynthesis process that converts carbon dioxide and water into glucose [17]. The adaxial side of the leaf is flat, while the abaxial side is characterized by ridges. The leaf epidermis layer, together with the internal tissues, controls the movement of water, light and carbon dioxide into the leaf and thus maintain an optimum temperature [18]. The hydrophobic nature of epidermis cells also helps to reduce water evaporation. The thick cuticle layer on the surface of the leaf is mainly composed of cutin, lignin, silica, waxes and a mixture of other cell wall materials [19]. There are relatively few stomata per unit of leaf area, aligned parallel to the long axis of the leaf, which are small and situated mainly on the abaxial surface of the leaves in depressed channels (Fig. 1e and 1f). Because of the smaller stomata size, deep and protected nature by a heavy coat of waxy trichomes, the plant has a very low rate of transpiration [20]. The leaf surfaces also show some impurities. The fiber surface is rough and uneven, which offers a large number of anchorage points and a good fiber-resin mechanical interlocking, and thus, provides a good adhesion to the matrix in a composite structure.

Anatomical features

Figure 2 shows the transverse section of pineapple leaf comprises of epidermis, xylem, phloem and parenchyma cells. The epidermis cell has an elongated shape without an intercellular space having one layer of a thick wall, which are common in monocots [17]. This layer protects the leaf against dehydration, intense sunlight, mechanical stress, as well as predation by herbivores. The outer epidermal cell wall resembles other primary cell walls in its composition but is thickened to the point where it comprises a substantial fraction in its outer layers with the cutin and waterproofed waxes [21]. The elongated palisade parenchyma is located under the epidermis

layer. It is arranged in a few layers, indicating that the plant receives strong sunlight. This cell contains chloroplasts and is the main photosynthesis tissue of the leaf. The spongy mesophyll cells have an open and net structure and are quite packed with limited intercellular spaces. The mesophyll cell is involved in oxygen, carbon dioxide and water vapor transportation. The vascular bundle is surrounded by the mesophyll cells, which are seen in Fig. 2b. The bundle consists of two fiber caps that consist of xylem and phloem that support the leaf and protect the transportation tissues inside the bundle [22].

Cell wall ultrastructure

The PALF cell wall architecture is depicted in Fig. 3. The fibers have a ribbon-like structure with very thick cell walls, including a narrow and elongated lumen. A similar description was also given by Mishra *et al.* [23]. The primary wall is clearly seen in the multilayered cell wall structure. The S_1 layer also shows brighter colors that help to distinguish the layer from the middle lamella. As usual, the S_2 layer is thicker than S_1 and S_3 layer (Table 1) and clearly dominates the secondary wall of the fiber. A very thin S_3 layer was found, which covers the inner cell wall layer. The parenchyma cells have only a primary

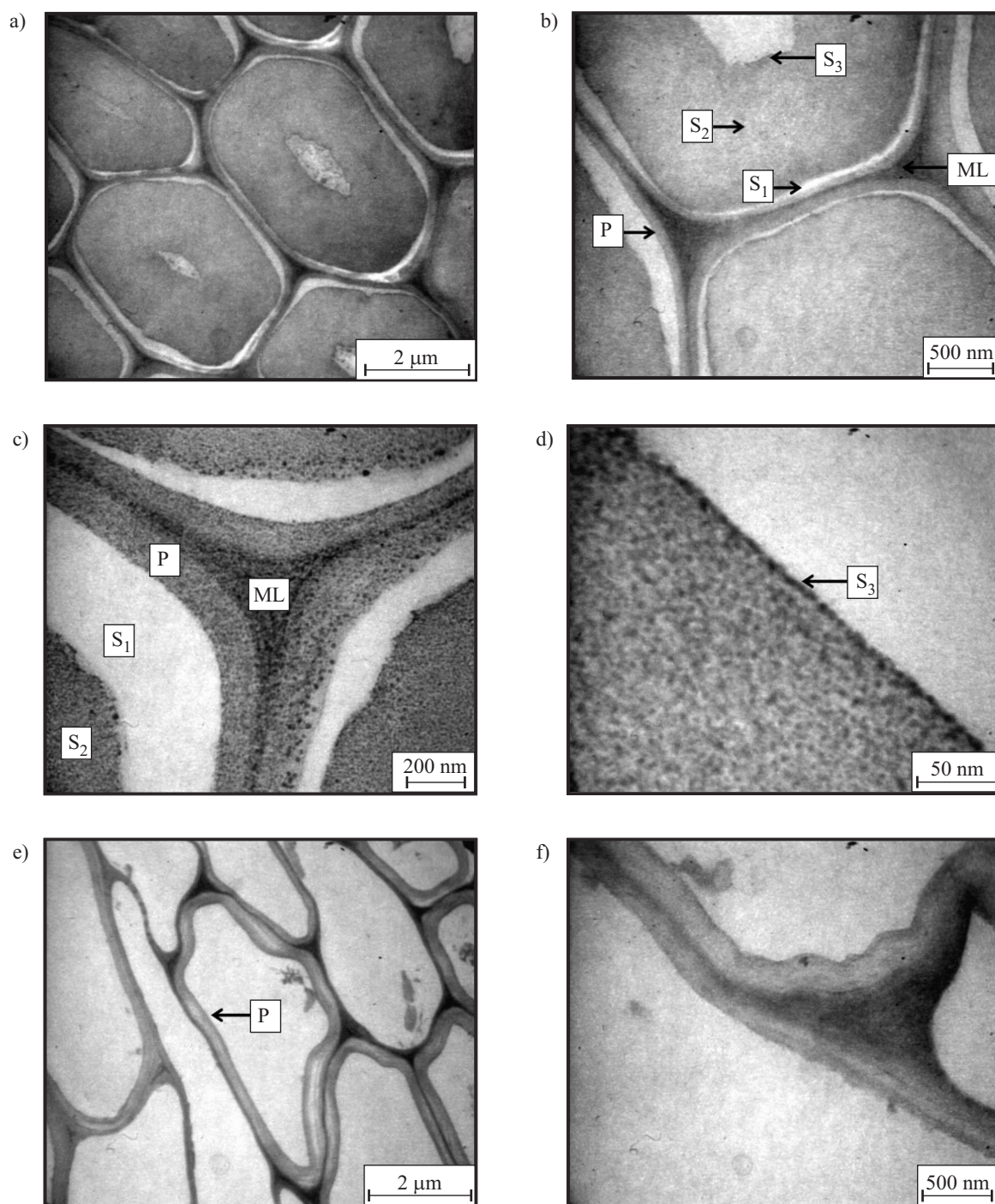


Fig. 3. TEM micrographs of pineapple leaf transverse sections showing the multilayered cell wall ultrastructure under low and high magnifications; P – primary wall, ML – middle lamella; S_1 , S_2 , S_3 – secondary wall

Table 1. Thickness of different morphological regions of plant fibers

| Morphological region | Width, μm^* (standard deviation) |
|----------------------|---|
| P | 0.118 (0.039) |
| S_1 | 0.148 (0.068) |
| S_2 | 1.192 (0.241) |
| S_3 | 0.016 (0.004) |

*) Fifty measurements were made and the results reflect the calculated means.

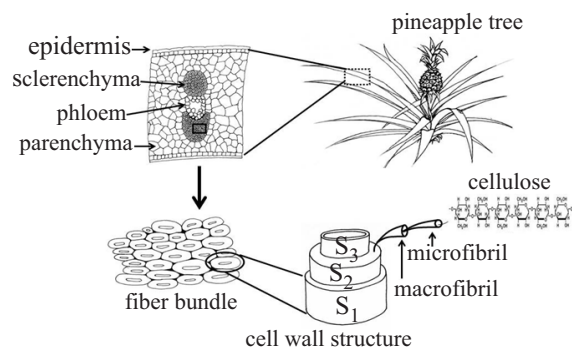


Fig. 4. Schematic illustration of the pineapple leaf structure

cell wall (Fig. 3e and 3f). It was found that cell wall thickness varied significantly ($p < 0.05$) in PALF (Table 2). The arrangement of the parenchyma cells was quite compact with very limited intercellular spaces. This adaptation is well served to the fact that this plant is grown in tropical regions. Fewer intercellular spaces reduce water loss by shrinking the leaf area. The cell wall layers form a composite with different abilities for plastic deformation and load bearing capacity. A schematic illustration of the cell wall organization of pineapple leaf is depicted in Fig. 4.

Table 2. Analysis of variance (ANOVA) for the thickness of plant cell walls of PALF fibers

| Variance | Sum of squares | DF | Mean square | F value | P value |
|----------|----------------|----|-------------|---------|---------|
| PALF | 45.68 | 3 | 15.23 | 945.52 | 0*) |

*) Indicated significance at 0.05 % level of probability.

Lignin topochemical distribution in plant cell wall

Figure 5 shows the Raman spectra and band detection from different morphological regions of pineapple leaf cell wall. The Raman bands are attributed primarily to the major cell wall components including cellulose, hemicelluloses and lignin. Band assignments to the pure model components have been assigned according to previous research on Raman spectra [10, 24, 25]. The band height indicates the concentration of cell wall components, *i.e.* the higher the band height, the greater the cell wall component concentrations. The band around 1600 cm^{-1} is attributed to the symmetric stretching of aromatic rings whereas the band around 2930 cm^{-1} is ascribed to lignin and carbohydrates [26]. The high intensities in the Raman spectra were observed for the cell corner (CC), indicating a higher lignin content at the CC compared to other areas. However, the amount of lignin in the secondary wall (SW) is greater compared to the combined middle lamella (CML) and CC because of the largest volume of SW (Table 1). Figure 6 shows the summary of

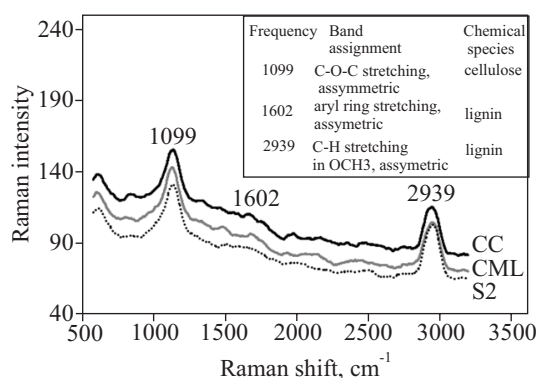


Fig. 5. Average Raman spectra acquired from the cell corner (CC), combined middle lamella (CML) and S_2 layer of the cell wall of PALF and their band assignments

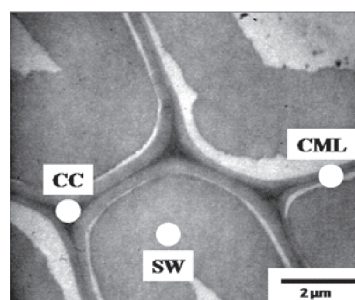


Fig. 6. SEM-EDX analysis of PALF by point analysis

| Analytical point | CC | CML | SW |
|------------------|------|------|------|
| 1 | 45.8 | 38.6 | 36.3 |
| 2 | 43.5 | 41.1 | 38.3 |
| 3 | 43.6 | 39.7 | 37.0 |
| 4 | 47.0 | 42.3 | 38.3 |
| 5 | 43.9 | 40.2 | 35.7 |
| 6 | 45.8 | 43.5 | 38.8 |
| 7 | 44.6 | 39.0 | 36.8 |
| 8 | 42.6 | 39.1 | 39.9 |
| 9 | 42.0 | 39.0 | 34.2 |
| 10 | 44.6 | 41.3 | 38.5 |
| Average | 44.3 | 40.3 | 37.3 |
| S.D | 1.4 | 1.5 | 1.6 |
| Ratio | 1.2 | 1.1 | 1.0 |

the SEM-EDX examination of pineapple leaf fiber by point analysis. During the analysis, the electron beam was kept fixed for a certain period in a selected morphological region (CML, CC and SW). The X-ray counts of Mn-K for various cell wall regions confirm that the largest lignin concentrations were found at the CC. The observations of this study fits with other studies on cell wall lignification of trees and monocotyledonous species [6, 27–29]. According to Fergus *et al.* [30], CML typically contains more than 50 % lignin concentration (w/w) while the S_2 region contains only about 20 %. This topochemical distribution is very important for the conversion of these fibers into nanocellulose, bio-fuels and bio-composites.

CONCLUSIONS

Pineapple leaf fiber has the potential to hold an important position among the natural fibers for its utilization in biocomposites and bio-fuel. However, the fibers need to be studied extensively for their efficient utilization. This study was performed to characterize the pineapple leaf fibers as a first step of these extensive studies. The pineapple leaf consists of sclerenchyma, vessel, phloem and parenchyma cells. The fiber surface is rough and irregular, composed of waxes and other encrusting substances including hemicelluloses, lignin and cellulose. The fiber has a nanocomposite structure consisting of primary wall and secondary wall (S_1 , S_2 , and S_3). The secondary wall dominates the cell wall structure. The lignin distributions in different morphological regions show that the cell corner has the highest concentration of lignin. Thus, all the information provided by the present study are very important for the efficient production of fibers and cellulose nanofibers for fabricating composites and biofuels.

ACKNOWLEDGMENT

The authors would like to thank the Universiti Sains Malaysia (USM), Penang, Malaysia, for providing Research Grant, No.: RUI- 1001/PTEKIND/814133 as a financial support.

REFERENCES

- [1] Ragauskas A.J., Williams C.K., Davison B.H., Britovsek G., Chairney J. *et al.*: *Science* **2006**, *311*, 484.
<http://dx.doi.org/10.1126/science.1114736>
- [2] Lau K.-T., Ho M.-P., Au-Yeung C.-T., Cheung H.-Y.: *Int. J. Smart Nanomater.* **2010**, *1*, 13.
<http://dx.doi.org/10.1080/19475411003589780>
- [3] Eudes A., George A., Mukherjee P., Kim J.S., Pollet B. *et al.*: *Plant Biotechnol. J.* **2012**, *10*, 609.
<http://dx.doi.org/10.1111/j.1467-7652.2012.00692.x>
- [4] Abdul Khalil H.P.S., Siti Alwani M., Mohd Omar M.: *Bio-Resources* **2006**, *1*, 220.
- [5] Wan Nadirah W.O., Jawaid M., Al Masri A.A., Khalil H.A., Suhaily S., Mohamed A.: *J. Polym. Environ.* **2012**, *20*, 404.
<http://dx.doi.org/10.1007/s10924-011-0380-7>
- [6] Li Z., Zhai H., Zhang Y., Yu L.: *Ind. Crops Prod.* **2012**, *37*, 130.
<http://dx.doi.org/10.1016/j.indcrop.2011.11.025>
- [7] Ma J., Yang G., Mao J., Xu F.: *Ind. Crops Prod.* **2011**, *33*, 358.
<http://dx.doi.org/10.1016/j.indcrop.2010.11.009>
- [8] Conrad K.: *Bioresour. Technol.* **2008**, *99*, 8476.
<http://dx.doi.org/10.1016/j.biortech.2007.08.088>
- [9] Agarwal U.P., McSweeney J.D., Ralph S.A.: *J. Wood Chem. Technol.* **2011**, *31*, 324.
<http://dx.doi.org/10.1080/02773813.2011.562338>
- [10] Hänninen T., Kontturi E., Vuorinen T.: *Phytochemistry* **2011**, *72*, 1889.
<http://dx.doi.org/10.1016/j.phytochem.2011.05.005>
- [11] Perera P.N., Schmidt M., Chiang V.L., Schuck P.J., Adams P.D.: *Anal. Bioanal. Chem.* **2012**, *402*, 983.
<http://dx.doi.org/10.1007/s00216-011-5518-x>
- [12] Agarwal U.P., Weinstock I.A., Atalla R.H.: *Tappi J.* **2003**, *2*, 22.
- [13] Mohamed A., Sapuan S., Shahjahan M., Khalina A.: *J. Food Agric. Environ.* **2009**, *7*, 235.
- [14] Ghosh S., Dey S.: *J. Inst. Eng.* **1983**, *16*, 23.
- [15] Arib R.M.N., Sapuan S.M., Ahmad M.M.H.M., Paridah M.T., Khairul Zaman H.M.D.: *Mater. Des.* **2006**, *27*, 391.
<http://dx.doi.org/10.1016/j.matdes.2004.11.009>
- [16] Sapuan S.M., Mohamed A.R., Siregar J.P., Ishak M.R.: "Pineapple Leaf Fibers and PALF-Reinforced Polymer Composites" in: „Cellulose Fibers: Bio- and Nano-Polymer Composites: Green Chemistry and Technology” (Eds. Sushel Kalia, Kaith B.S., Inderjeet Kaur), Springer, Berlin Heidelberg 2011.
- [17] Mauseth J.D.: "Plant anatomy", Benjamin/Cummings Publ. Co., California 1988.
- [18] Kang J., Dengler N.: *Int. J. Plant Sci.* **2004**, *165*, 231.
<http://dx.doi.org/10.1086/382794>
- [19] Dickison C.E.: "Integrative plant anatomy", Academic Press, London 2000.
- [20] Bartholomew D.P., Paull R.E., Rohrbach K.G.: "The pineapple: botany, production, and uses", CABI Publishing, London 2003.
- [21] Jarvis M.C.: *Food Hydrocolloids* **2011**, *25*, 257.
<http://dx.doi.org/10.1016/j.foodhyd.2009.09.010>
- [22] MacAdam J.W.: "Structure and function of plants", John Wiley & Sons Ltd., USA 2011.
- [23] Mishra S., Mohanty A.K., Drzal L.T., Misra M., Hinrichsen G.: *Macromol. Mater. Eng.* **2004**, *289*, 955.
<http://dx.doi.org/10.1002/mame.200400132>
- [24] Agarwal U.P., Ralph S.A.: *Appl. Spectros.* **1997**, *51*, 1648.
<http://dx.doi.org/10.1366/0003702971939316>
- [25] Gierlinger N., Schwanninger M.: *Plant Physiol.* **2006**, *140*, 1246. <http://dx.doi.org/10.1104/pp.105.066993>
- [26] Sun L., Simmons B.A., Singh S.: *Biotechnol. Bioeng.* **2011**, *108*, 286. <http://dx.doi.org/10.1002/bit.22931>
- [27] Richter S., Müssig J., Gierlinger N.: *Planta* **2011**, *233*, 763.
<http://dx.doi.org/10.1007/s00425-010-1338-z>
- [28] Agarwal U.P.: *Planta* **2006**, *224*, 1141.
<http://dx.doi.org/10.1007/s00425-006-0295-z>
- [29] Fromm J., Rockel B., Lautner S., Windeisen E., Wanner S.: *J. Struct. Biol.* **2003**, *143*, 77.
[http://dx.doi.org/10.1016/S1047-8477\(03\)00119-9](http://dx.doi.org/10.1016/S1047-8477(03)00119-9)
- [30] Fergus B., Procter A., Scott J., Goring D.: *Wood Sci. Technol.* **1969**, *3*, 117. <http://dx.doi.org/10.1007/BF00639636>

Received 1 X 2013.